A Theoretical Study on the Reaction Mechanism of the Gas-Phase Decomposition of NO by NH_3^+ and NH_4^+

Yuka Kobayashi,* Nobuo Tajima, and Kimihiko Hirao

Department of Applied Chemistry, Graduate School of Engineering, The University of Tokyo, Hongo 7-3-1, Bunkyo-ku, Tokyo 113-8656, Japan

Received: December 23, 1999; In Final Form: May 22, 2000

High level ab initio calculations have been performed to study the mechanism of NO decomposition by NH_3^+ and NH_4^+ in the gas phase, $NH_3^+ + NO \rightarrow N_2 + H_3O^+$ and $NH_4^+ + NO \rightarrow N_2H + H_3O^+$. The density functional theory was used to search for possible reaction pathways. The multiconfigurational second-order perturbation (CASPT2) method is applied to the most energetically favorable pathways to obtain more accurate energy diagrams. NO reacts with NH_3^+ and NH_4^+ by producing nitrogen−nitrogen bound complexes and by donating protons/hydrogens to the O atom to weaken the N−O bond and to tighten the N−N bond. Maximum activation energies for these reactions were estimated as 55.3 and 77.3 kcal/mol.

1. Introduction

Selective catalytic reduction (SCR) of NO by NH_3 is a very important reaction from an environmental point of view.[1] The process is widely used because it enables removal of NO under mild conditions at low cost. NO is catalytically decomposed by NH_3 into N_2 and H_2O, and the industrial catalysts are based on a V_2O_5 surface, e.g. $V_2O_5-WO_3$ and $V_2O_5-MoO_3$ supported by TiO_2.[2] It is strongly desired that the reaction mechanisms and the roles of these catalysts be clarified to improve the efficiency of NO decomposition. Several groups have proposed that SCR proceeds in the same way as NO decomposition by NH_3 in the gas phase.[3] In the gas phase, the reaction proceeds via an intermediate, NH_2NO. The activated species reacting directly with NO is NH_2, which is produced from thermally decomposed NH_3,

$$NH_3 \rightarrow NH_2 + H \quad NH_2 + NO \rightarrow NH_2NO \rightarrow N_2 + H_2O \qquad (1)$$

The importance of this mechanism on the catalyst is still being debated. The NH_2NO is detected as a major intermediate at temperatures above that of the SCR conditions (>300 °C); however, it has never been observed under SCR conditions (<250 °C).[4] This suggests that the active molecule, NH_2, is not involved in SCR, and the mechanism of catalytic decomposition of NO may differ entirely from the gas-phase reaction. It has been proposed that the active species reacting with NO in the SCR must be NH_3^+ or NH_4^+ instead of NH_2,

$$\begin{aligned}(V^{5+}{=}O) + (V_4^{+}{-}O)^{-}\cdots NH_4^{+} + NO &\rightarrow (V^{4+}{-}OH) + (V^{4+}{-}O)^{-}\cdots NH_3^{+} + NO \\ &\rightarrow (V^{4+}{-}OH) + (V^{4+}{-}O)^{-}\cdots NH_3^{+}NO \\ &\rightarrow (V^{4+}{-}OH) + (V^{4+}{-}OH) + N_2 + H_2O\end{aligned} \qquad (2)$$

$$\begin{aligned}(V^{5+}{=}O) + (V^{4+}{-}OH) + NH_3 + NO &\rightarrow (V^{5+}=O) + (V^{4+}{-}O)^{-}\cdots NH_4^{+} + NO \\ &\rightarrow (V^{4+}{-}OH) + (V^{4+}{-}OH) + N_2 + H_2O\end{aligned} \qquad \text{(ref 6)} \quad (3)$$

where $(V^{5+}{=}O)$ and $(V^{4+}{-}O)^{-}$ are the oxidized and reduced sites of the V_2O_5 surface, respectively. There is little experimental evidence to support these reactions.

In this paper, as an approach to understanding the SCR mechanism, we have studied the NO decomposition reactions by NH_3^+ and NH_4^+ in the gas phase. The mechanism of these gas-phase reactions has never been examined. We report reaction pathways, intermediate products, and rate-determining steps obtained by high level ab initio calculations for the following NO decomposition reactions:

$$NH_3^+ + NO \rightarrow N_2 + H_3O^+ \qquad (4)$$

$$NH_4^+ + NO \rightarrow N_2H + H_3O^+ \qquad (5)$$

2. Computational Details

When the NO decomposition reactions 4 and 5 take place, an N−O triple bond and three N−H bonds are broken, and an N−N triple bond and three O−H bonds are formed. The change in the number of X−H bonds is achieved by proton/hydrogen transfers from NH_3 or NH_4^+ to the O atom, and this leads to the weakening and finally to the cleaving of the N−O bond. The cleaving of N−H and N−O bonds leads to an increase in free valences on the two N atoms, and the N−N bond is produced and strengthened. Thus, reactions 4 and 5 will be mainly driven by the proton/hydrogen transfer process. Because of the variation in the proton/hydrogen transfer sites, many reaction pathways are possible. Among them, the most energetically favorable pathway is regarded as the probable one.

For the purpose of searching for the most favorable reaction pathways, equilibrium and transition state structures for reactions

10.1021/jp9944637 CCC: $19.00
Published on Web 07/01/2000

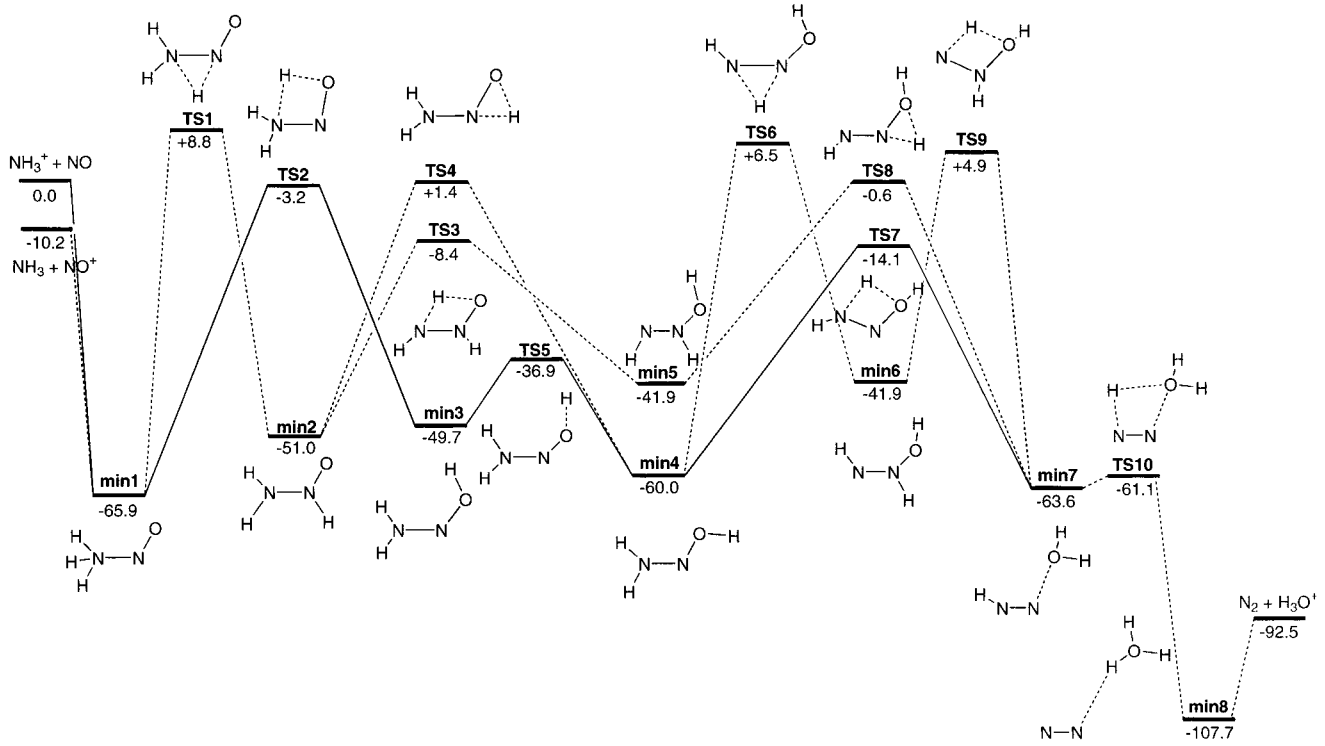

Figure 1. Energy diagram for the NO decomposition reaction $NH_3^+ + NO \rightarrow N_2 + H_3O^+$, calculated by BLYP/cc-pVDZ. Energies are in kcal/mol and relative to the reactants $NH_3^+ + NO$.

4 and 5 are determined. Density functional theory (DFT), employing Becke's exchange[7] and Lee−Yang−Parr's correlation functionals (BLYP),[8] was used with cc-pVDZ [9] in these calculations. Only for the most favorable pathway for each reaction, the geometries are reoptimized at the level of the complete active space self-consistent-field (CASSCF) method[10] using cc-pVDZ. The active space consists of 10 electrons distributed among 10 orbitals (10,10) for reaction 4, and (7,7) for reaction 5. All geometries have been fully optimized without symmetry constraints. Each transition state is verified to connect with two minima before and after the transition state. That is, the transition state geometry is slightly deformed in accord with the transition vector with an imaginary frequency and it is confirmed by subsequent optimizations that the transition state leads to the minima depicted in Figures 3 and 6. Using the optimized geometries, single-point calculations were carried out to estimate the energies using the multiconfigurational second-order perturbation (CASPT2) method[11] with aug-cc-pVDZ.[12] The active spaces were (10,10) and (11,11) for reactions 4 and 5, respectively. In this system, it is rather difficult to keep the active electrons and orbitals consistent throughout the entire reaction paths. The active space was chosen to include seven electrons distributed among seven orbitals (7,7) for NO in both reactions. In addition, three electrons in three orbitals (3,3) for NH_3^+ and four electrons in four orbitals (4,4) for NH_4^+ were chosen as active.

B3LYP[13] optimization with aug-cc-pVDZ was performed only along the most favorable paths in order to compare with CASPT2 results. The DFT calculations were performed using Gaussian 98 packages.[14] Geometry optimization by CASSCF was carried out with HONDO8,[15] and CASPT2 single-point energy calculations with MOLCAS.4.1.[16]

3. Results and Discussion

Reaction: $[NH_3^+ + NO \rightarrow N_2 + H_3O^+]$. Several reaction pathways were determined by the BLYP method and are summarized in Figure 1. The first process in NO decomposition, which is common to all the pathways, is a barrierless N−N association to NH_3NO^+ (**min1**), and this process is followed by multiply branched processes of proton or hydrogen atom transfers and isomerizations of $[NH_3NO^+]$ molecules. As seen in the energy diagram, all of the proton or hydrogen atom transfer processes need fairly large activation energies. Hence, the barrier heights for these processes determine the preferred pathways. The transition state structures for proton or hydrogen transfer processes with four-membered rings (**TS2**, **TS3**, **TS7**, and **TS9**) are relatively stable compared with those with three-membered rings (**TS1**, **TS4**, **TS6**, and **TS8**). The most favorable reaction pathway (solid line in Figure 1) is obtained by connecting those transition states.

Figure 2 shows the energy diagram for the most favorable pathway computed by CASPT2, CASSCF, and B3LYP. Figure 3 shows geometries optimized by CASSCF. The first N−N interacting intermediate, **min1**, is an ion−molecule complex of NH_3 and NO^+ which is produced by an electron transfer from NO to NH_3^+. In the complex, NH_3 no longer has the planar geometry observed in NH_3^+, and the N−O distance is substantially shortened compared with that in free NO. The two nitrogen atoms interact through the lone pair of NH_3 and the unoccupied π^* orbital of NO^+. This N−N coordinate bond accounts for the quite long bond length of 2.372 Å. **Min1** changes to an intermediate with tight N−N bond, **min3**, via **TS2**. In the earlier stage of this process, the complex changes its nature back to NH_3^+−NO by which N═O and N−N bonds are produced. In the later stage, a proton transfers from N1 to O3 by which the N−H and N−O bonds are reorganized to N−N and O−H bonds, and the sp^2 orbital of O3 changes to sp^3. Since the N2−O3 bond loses and the N−N bond gains π-bonding characteristics, the former becomes relatively weak and the latter becomes strong to make the planar geometry of **min3**. **Min3** takes a *cis*-form around the terminal N−O bond, and isomerizes to the more stable *trans*-form, **min4**. **Min4** undergoes a hydrogen atom

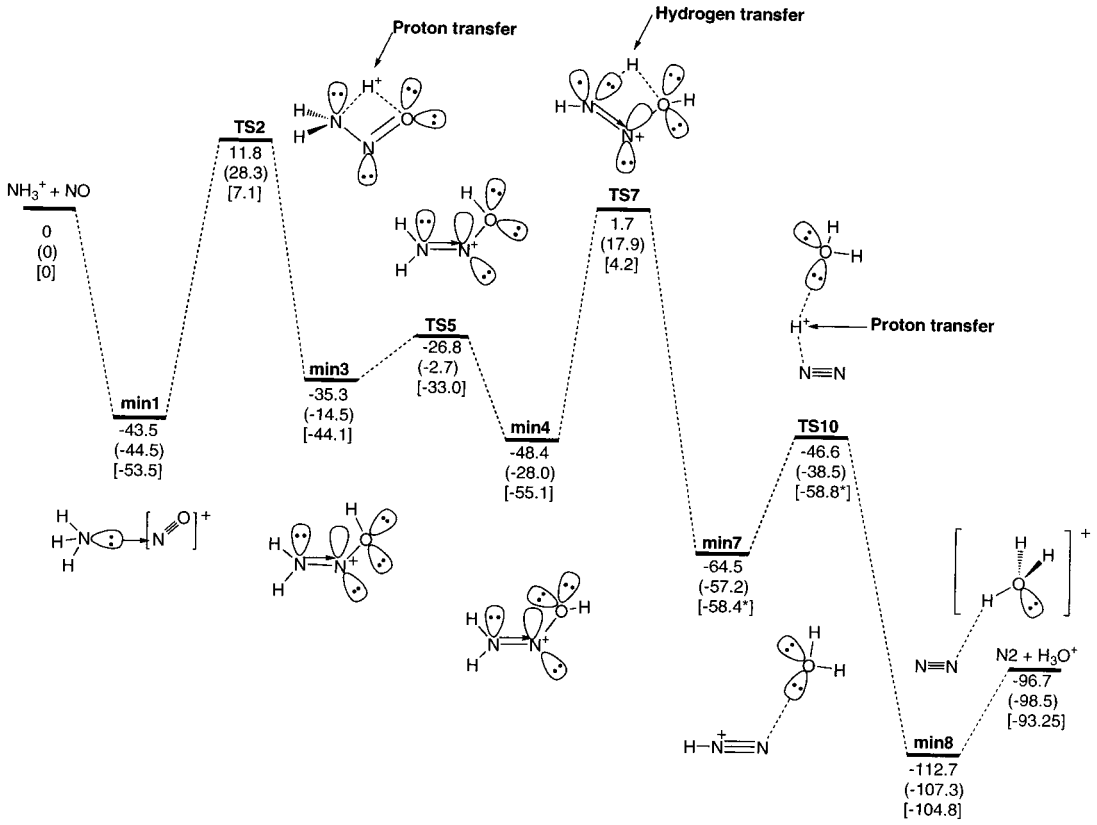

Figure 2. Energy diagram for the NO decomposition reaction $NH_3^+ + NO \rightarrow N_2 + H_3O^+$. Energies are in kcal/mol and relative to the reactants $NH_3^+ + NO$. Top, middle and bottom values were calculated by CASPT2(10,10)/aug-cc-pVDZ//CASSCF(10,10)/cc-pVDZ, CASSCF(10,10)/aug-cc-pVDZ//CASSCF(10,10)/cc-pVDZ, and B3LYP/aug-cc-pVDZ//B3LYP/aug-cc-pVDZ. The states marked with a star are calculated by B3LYP/aug-cc-pVDZ//B3LYP/cc-pVDZ. An arrow means a partial bond formed by charge transfer.

TABLE 1: N−N and N−O Bond Distances Optimized by CASSCF and B3LYP in Angstrom in the Reaction 4[a]

	N−N distance	N−O distance
min1	2.372(2.019)	1.068(1.104)
Ts2	1.488(1.452)	1.229(1.214)
min3	1.265(1.258)	1.310(1.287)
Ts5	1.265(1.245)	1.309(1.341)
min4	1.259(1.253)	1.324(1.300)
Ts7	1.218(1.224)	1.494(1.457)
min7	1.098(1.107)	2.902(2.295)
Ts10	1.098(1.101)	3.166(2.499)
min8	1.112(1.102)	3.923(2.678)

[a] B3LYP values are in parentheses.

transfer from N1 to O3 at **TS7**. In the process, the hydrogen atom transfers to O3 to construct sp and sp^3 orbitals on the two nitrogen atoms and oxygen atom, respectively. This process completes the formation of an N≡N triple bond and cleavage of an N−O bond, and the product **min7** is a complex of N_2H^+ and H_2O. The H_2O abstracts H^+ from N_2H^+, in the structure **min8** N_2 and H_3O^+ interact weakly. The changes of electronic states, as well as the nature of the molecules, are well reflected in the bond length. The N−N and N−O bond distances optimized by CASSCF and B3LYP are summarized in Table 1.

There is a considerable difference between the relative energies by CASSCF and CASPT2. The differences are large in the structures **TS2**-**TS7**, which indicates that dynamical correlations are important in estimating the energies of the N−N bonding molecules of this system. However, their activation energies agree comparatively well except for the first hydrogen transfer process. As a whole, the dynamical correlation correction by CASPT2 decreases the activation energies of CASSCF. Comparing the energies by CASPT2 and B3LYP in Figure 2, B3LYP is proved to give slightly higher activation barriers than CASPT2, although DFT is generally considered to underestimate the energy of a transition state.[17] The quite different picture is found in the description of **TS10**. The geometry of **min7** and **TS10** by B3LYP/aug-cc-pVDZ is not converged so that the structures optimized by B3LYP/cc-pVDZ are adopted for the energy estimation with aug-cc-pVDZ basis sets. Then the energy of **TS10** becomes lower than that of **min7**. BLYP also yields very low barrier height of 2.5 kcal/mol for **TS10** as shown in Figure 1. On the other hand, CASPT2 and CASSCF predict that the barrier is considerably higher, ca. 18 kcal/mol. This difference may come from the poor description of DFT on the weakly bound complex. According to the CASPT2 results, the first proton-transfer process has an activation barrier of 55.3 kcal/mol, which is the rate-determining step. The hydrogen transfer and the second proton-transfer processes require 50.1 and 17.9 kcal/mol, respectively. The activation barrier corresponding to the internal rotation is smaller than those of proton/hydrogen transfers.

Reaction: $[NH_4^+ + NO \rightarrow N_2H + H_3O^+]$. Using the same strategy as that used for reaction 4, reaction pathways were examined by BLYP calculations. The energy diagram is shown in Figure 4. In contrast to reaction 4, the N−N bonding processes need large activation energies and are comparable or more difficult than the proton/hydrogen transfer processes. There are two pathways to form the first N−N bond intermediate from NO and NH_4^+: the negatively charged O atom of NO abstracts a proton from NH_4^+ to produce **min1,** and the π^* orbital in NO as HOMO accepts a hydrogen atom to produce **min2**. The latter reaction is preferable because the starting complex **min2** is more stable than **min1** and the activation barrier is smaller

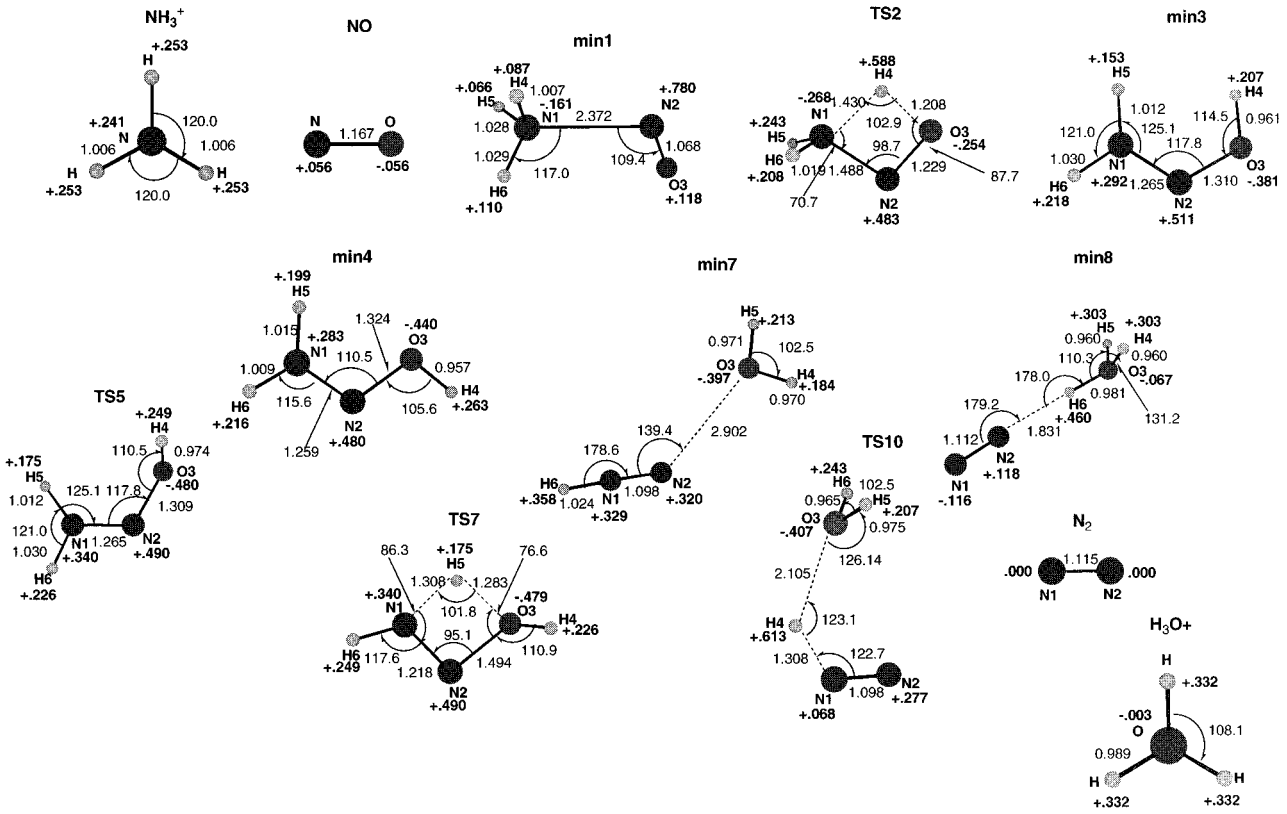

Figure 3. Geometries of equilibrium and transition state structures determined by CASSCF(10,10)/cc-pVDZ for the NO decomposition reaction $NH_3^+ + NO \rightarrow N_2 + H_3O^+$ (bond lengths and angles in angstrom and degree, respectively). Bold values indicate net charge on each atom.

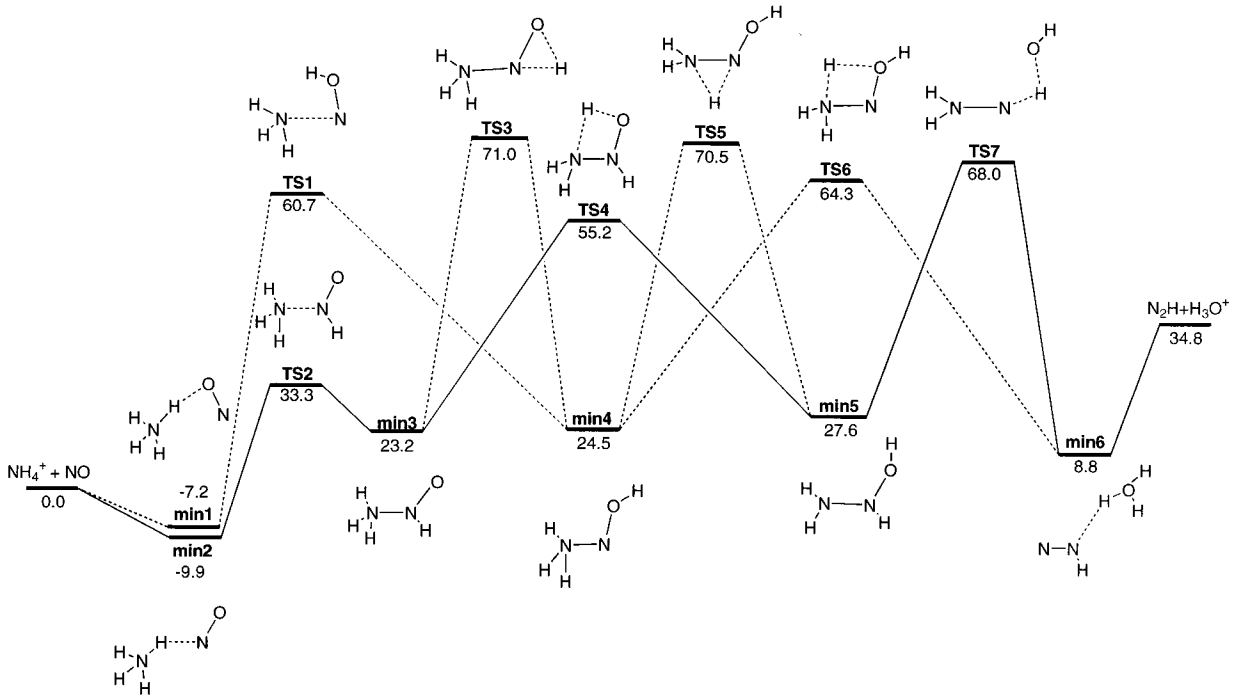

Figure 4. Energy diagram for the NO decomposition reaction $NH_4^+ + NO \rightarrow N_2H + H_3O^+$, calculated by BLYP/cc-pVDZ. Energies are in kcal/mol and relative to the reactants $NH_4^+ + NO$.

than that of the former. This N−N bonding reaction followed by proton/hydrogen transfer reactions produces the reaction pathway depicted by a solid line in Figure 4.

The energy diagram by CASPT2 for the most favorable pathway is shown in Figure 5 and the optimized structures are given in Figure 6. The first intermediate, **min2**, is an ion−molecule complex of NH_4^+ and NO, where one of the ammonium hydrogens interacts with atom N2 of NO. In **TS2** a hydrogen atom transfers to N2, and N1 and N2 come closer and form **min3**. The N−N distance in **min3**, 1.464 Å, is quite normal for an N−N single bond. The electronic structure, however, indicates a fractional bond order for this N−N linkage. The N−N bond in **min3** consists of a doubly occupied σ and a singly occupied σ^* orbital, both arising from the lone pair

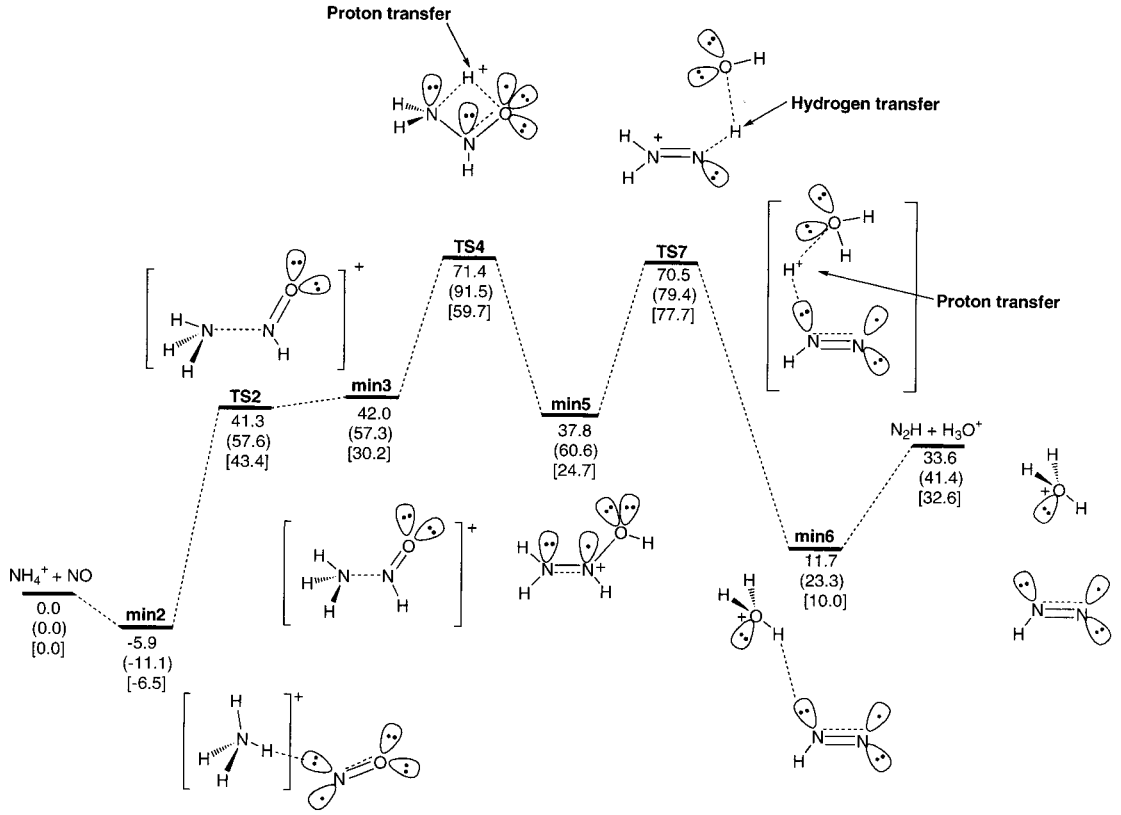

Figure 5. Energy diagram for the NO decomposition reaction $NH_4^+ + NO \rightarrow N_2H + H_3O^+$. Top, middle and bottom values were calculated by CASPT2(11,11)/aug-cc-pVDZ//CASSCF(7,7)/cc-pVDZ, CASSCF(11,11)/aug-cc-pVDZ//CASSCF(7,7)/cc-pVDZ, and B3LYP/aug-cc-pVDZ//B3LYP/aug-cc-pVDZ. An arrow means a partial bond formed by charge transfer.

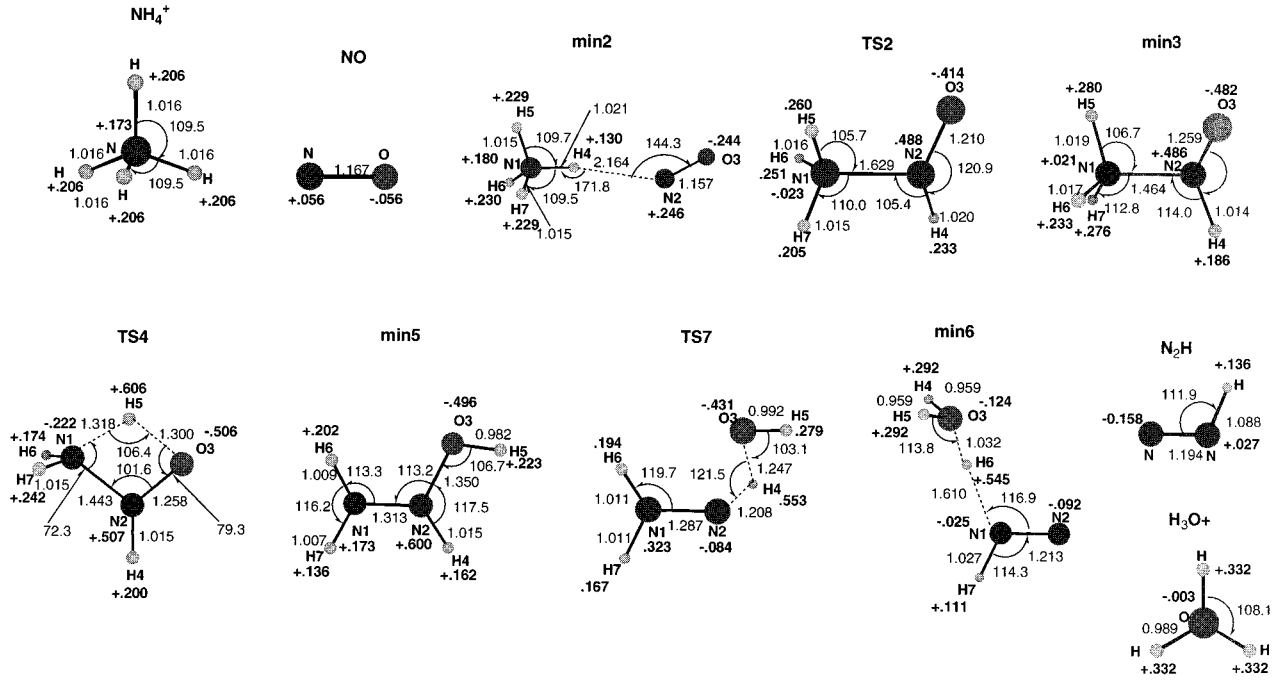

Figure 6. Geometries of equilibrium and transition state structures determined by CASSCF(7,7)/cc-pVDZ for the NO decomposition reaction $NH_4^+ + NO \rightarrow N_2H + H_3O^+$ (bond lengths and angles in angstrom and degree, respectively). Bold values indicate net charge on each atom.

orbitals of NH_3 and HNO^+. According to B3LYP/aug-cc-pVDZ optimization, N−N bond length in **TS2** is 2.347 Å, which is quite longer than that of CASSCF. The structure has one imaginary frequency of 917.7*i* cm^{-1}. The N−N bond in **min3** is 1.562 Å, which is slightly longer compared to that of CASSCF. From this intermediate, first proton transfer takes place in **TS4**, and the N−H and N═O bonds are reorganized to N−N and N−O−H. The N−N and N−O bond lengths computed by CASSCF are 1.313 and 1.350 Å, respectively, indicating that the formal bond order of each will be 1.5 and 1.0. In **TS7**, a hydrogen atom transfers to the O3 atom first, and then the H_2O produced abstracts a proton from N1. In the final intermediate, **min6**, H_3O^+ is formed and the proton of H_3O^+ interacts weakly with an N atom of N_2H. The N−N and

TABLE 2: N−N and N−O Bond Distances Optimized by CASSCF and B3LYP in Angstrom in the Reaction 5[a]

	N−N distance	N−O distance
min2	3.177(3.023)	1.157(1.146)
Ts2	1.629(2.347)	1.210(1.151)
min3	1.464(1.562)	1.259(1.230)
Ts4	1.443(1.419)	1.258(1.293)
min5	1.313(1.323)	1.350(1.358)
Ts7	1.287(1.301)	1.582(1.588)
min6	1.213(1.192)	3.329(2.527)

[a] B3LYP values are in parentheses.

N−O bond distances optimized by CASSCF and B3LYP are summarized in Table 2.

CASPT2 shows that the **TS2** energy at the CASSCF geometry is more stable than that of **min3**. There may exist a CASPT2 barrier to the connection of **min2** with **min3**. Even in this case the barrier height must be very low. Therefore, the process **min2 → min5** should be a one-step reaction. This is the rate-determining step, and the activation energy amounts to 77.3 kcal/mol. The proton-transfer process **min5 → min6** has an activation energy of 32.7 kcal/mol. The activation barriers predicted by B3LYP are again relatively high compared to those by CASPT2.

Compared with reaction system 4, this system has an excess electron arising from an excess hydrogen atom, and the excess electron gives rise to the antibonding character on the N−N−O linkage, mainly on N−N. Thus, the N−N bond is not as tight as that produced with reaction 4.

The calculated energy diagrams clarify the reactivities of NH_3^+ and NH_4^+ for the NO decomposition. As shown in Figure 2, NH_3^+ is active in the sense that it ionizes NO and produces the N···N associated complex **min1** without an energy barrier and with large exothermicity. Both NO and NH_3^+ have radical electrons on the nitrogen and the radicals react immediately once they meet. However, further reactions via proton/hydrogen transfers are high energy processes. It seems that NH_3^+ has difficulty in decomposing NO into products N_2 and H_3O^+ by itself. In contrast, NH_4^+ is quite inert to NO since only a weak electrostatic interaction in **min1** is possible unless a lot of energy is supplied to the system. The NH_4^+ seems too stable to react directly with NO as the N···N does not interact until NH_4^+ loses a proton and is activated. NH_3^+ is more efficient than NH_4^+ at decomposing NO: the activation energy for the former reaction is significantly smaller than that of the latter, 55.3 and 77.3 kcal/mol, respectively. This difference can be ascribed mainly to the different feasibilities in the N···N association.

The reactivities of NH_3^+ and NH_4^+ are characterized by comparison with the reactivity of NH_2, the active molecule in the gas-phase reaction. According to the theoretical study by Walch[3] using the MRCI method with basis sets of triple-ζ plus polarization quality, the reaction $NH_2 + NO \rightarrow N_2 + H_2O$ proceeds by the barrierless N−N bonding (exothermic by 44.0 kcal/mol) and H transfer processes (maximum barrier height 37.1 kcal/mol). NH_3^+ is less active than NH_2 in proton transfers, and NH_4^+ is much less active. This comparison indicates that the role of the catalyst in SCR is not explained simply by the formation of active molecules NH_3^+ or NH_4^+, otherwise the efficiency of NO decomposition would decrease in the presence of the catalyst.

In this study, we have not taken into account the interactions of intermediates and transition states with the catalyst surface, but it must play a crucial role in SCR. The reaction mechanisms on the catalyst as well as the formation of these active molecules will be studied by calculations using an appropriate model of the catalyst surface.

4. Conclusions

The mechanisms of NO decomposition with NH_3^+ and NH_4^+ have been studied, these species being proposed as activated molecules in SCR.[5,6] The most favorable pathway was determined by DFT calculations, and the energy profile was characterized by CASPT2 calculations. NH_3^+ was found to be reactive toward NO; NH_3^+ ionizes NO and produces N···N interacting complex **min1** without an energy barrier. However, the proton-transfer processes to complete the NO decomposition are high energy processes, of which the largest activation energy is 55.3 kcal/mol. NH_4^+ is much less reactive toward NO than NH_3^+; the N···N bond cannot be formed until NH_4^+ itself is activated. The maximum barrier height is estimated as 77.3 kcal/mol for the N−N bonding process **min2 → min5**. The energy barriers for reactions 4 and 5 suggest that NO is not decomposed easily by NH_3^+ and NH_4^+ in the absence of a catalyst.

Acknowledgment. This research was supported in part by a grant-in-aid for Scientific Research on Priority Areas "Molecular Physical Chemistry" from the Ministry of Education, Science, Sports and Culture of Japan, and by the grant from the Genesis Research Institute. One of the authors (N.T.) is indebted to the Japan Society for the Promotion of Science for a research fellowship.

References and Notes

(1) Henry, J. G.; Heinke, G. W. *Environmental Science and Engineering*; Prentice-Hall: Englewood Cliffs, NJ, 1989.
(2) Forzatti, P.; Lietti, L. *Heterog. Chem. Rev.* **1996**, *3*, 33.
(3) Walch, S.P. *J. Chem. Phys.* **1993**, *99*, 5295.
(4) Farber, M.; Harris, S. P. *J. Phys. Chem.* **1984**, *88*, 680.
(5) Topsøe, N. Y. *Science* **1994**, *265*, 1217.
(6) Miyamoto, A.; Kobayashi, A.; Inomata, M.; Murakami, Y. *J. Phys. Chem.* **1982**, *86*, 2945.
(7) Becke, A. D. *Phys. Rev.* **1988**, *A38*, 3098.
(8) Lee, S.; Yang, W.; Parr, R. G. *Phys. Rev.* **1988**, *B37*, 785.
(9) Dunning Jr., T. H. *J. Chem. Phys.* **1989**, *90*, 1007.
(10) Hegarty, D. Robb, M. A. *Mol. Phys.* **1979**, *38*, 1795.
(11) Andersson, K.; -Å Malmqvist, P.; Roos, B. O. *J. Chem. Phys.* **1992**, *96*, 1218.
(12) Kendall, R. A.; Dunning Jr., T. H.; Harrison, R. J. *J. Chem. Phys.* **1992**, *96*, 6769.
(13) Becke, A. D. *J. Chem. Phys.* **1993,** *98*, 5648.
(14) Frisch, M. J.; Trucks, G. W.; Schlegel, H. B.; Scuseria, G. E.; Robb, M. A.; Cheeseman, J. R.; Zakrzewski, V. G.; Montgomery, J. A., Jr.; Stratmann, R. E.; Burant, J. C.; Dapprich, S.; Millam, J. M.; Daniels, A. D.; Kudin, K. N.; Strain, M. C.; Farkas, O.; Tomasi, J.; Barone, V.; Cossi, M.; Cammi, R.; Mennucci, B.; Pomelli, C.; Adamo, C.; Clifford, S.; Ochterski, J.; Petersson, G. A.; Ayala, P. Y.; Cui, Q.; Morokuma, K.; Malick, D. K.; Rabuck, A. D.; Raghavachari, K.; Foresman, J. B.; Cioslowski, J.; Ortiz, J. V.; Stefanov, B. B.; Liu, G.; Liashenko, A.; Piskorz, P.; Komaromi, I.; Gomperts, R.; Martin, R. L.; Fox, D. J.; Keith, T.; Al-Laham, M. A.; Peng, C. Y.; Nanayakkara, A.; Gonzalez, C.; Challacombe, M.; Gill, P. M. W.; Johnson, B. G.; Chen, W.; Wong, M. W.; Andres, J. L.; Head-Gordon, M.; Replogle, E. S.; Pople, J. A. *Gaussian 98*, revision A.7; Gaussian, Inc.: Pittsburgh, PA, 1998.
(15) Dupuis, M.; Marquez, A.; Davidson, E. R. HONDO95.1 from CHEM-Station. IBM Corporation: Neighborhood Road, Hingston, NY 12401, 1995.
(16) Andersson, K.; Margareta, R. A.; Fülscher, M. P.; Karlström, G.; Lindh, R.; Malmqvist, P.; Neogrády, P.; Olsen, J.; Roos, B. O.; Sadlej, A. J.; Schütz, M.; Seijo, L.; Andrés, L. S.; Siegbahn, P. E. M.; Widmark, P. O. MOLCAS, version 4.1; Lund University: Sweden, 1997.
(17) Zhang, Y.; Yang, W.; *J. Chem. Phys.* **1998**, *109*, 2604.